2007 CEDAR - DASI Workshop
Eldorado Hotel
Santa Fe, New Mexico, USA
June 24 - 29, 2007

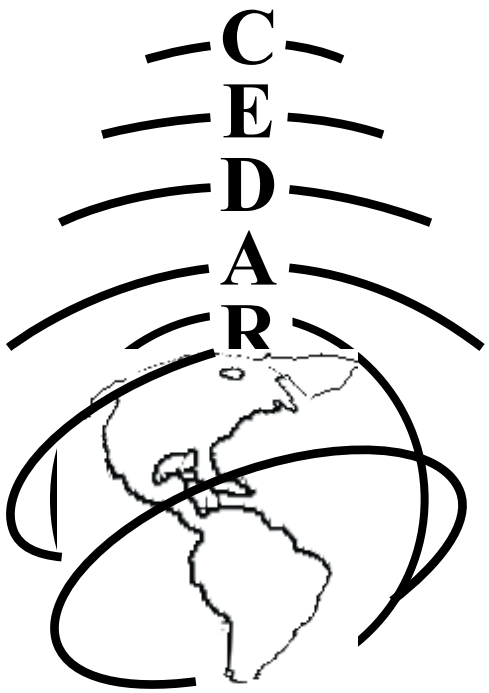

Tuesday CEDAR Poster Session Booklet
June 26

Table of Contents

I. Mesosphere or Lower Thermosphere General Studies

II. Mesosphere or Lower Thermosphere –Lidar

III. Yee Posters: MLT Climatology

IV. Polar MLT Aeronomy

V. Mesosphere or Lower Thermosphere – Tidal or Planetary Waves

VI. Mesosphere or Lower Thermosphere – Gravity Waves

VII. Sprites, Jets and Lightning

VIII. Stratosphere Studies and Below

IX. Instruments or Techniques for Middle Atmospheric Observation

Mesosphere or Lower Thermosphere General Studies

MLT-01 E-Region Ion Motion and Related Thermospheric Properties - by Ashley Wiren

Status of First Author: Student IN poster competition PhD

Authors: Ashley Wiren, ashley.wiren@colorado.edu, Jeff Thayer, jeffrey.thayer@colorado.edu

Abstract: The ion behavior in the polar ionosphere deviates from ExB plasma drift motion with descending altitude as the neutral gas density and wind exert a greater influence on the ion motion. The neutral gas density is directly proportional to the ion-neutral collision frequency which imposes a drag on the ions leading to a decrease in ion velocity magnitude and a rotation of the ion velocity vector towards the local electric field direction. Neutral gas winds will also alter the ion motion in a manner that depends on the ion-neutral vector relationship. The altitude where the deviation from ExB occurs is due to gas density and/or winds. Data from the Sondrestrom incoherent scatter radar are used to indicate the contribution from these neutral properties. The data indicate the potential to isolate the two effects enabling their impact and temporal evolution to be evaluated. The Global Ionosphere Thermosphere Model (GITM) will allow the separate effects of the neutral gas density and wind to be seen.

MLT-02 Long-term Meridional Neutral Wind Study over Arecibo using Incoerent Scaterring Radar - by Pedrina Terra Santos

Status of First Author: Non-student PhD

Authors: Pedrina Terra Santos, Sixto Gonzales, Nestor Aponte, Craig Tepley, Christiano Garnett Brum

Abstract: This work presents the results of a long-term meridional neutral wind study carried out at Arecibo (18.35oN, 66.75oW) from 1986 to 2006 (20 years of experiments). These winds were obtained indirectly from measurements of the ion velocities by means of the Incoherent Scattering Radar (ISR). The analyses presented here are performed only for the nighttime period (0 UT to 8 UT) and during geomagnetically quiet conditions. The ISR results are compared with the meridional neutral wind component obtained by 630nm Fabry-Perot Interferometer (FPI) and also with the model developed by Brum (2006), under same aeronomic conditions.

MLT-03 Behavior of the Neutral Wind Components over Arecibo during geomagnetically quiet conditions - by Christiano Garnett Brum – presented by Eva Robles

Status of First Author: Non-student

Authors: Christiano Garnett Marques Brum (Inpe/garnett@dae.inpe.br), Craig Tepley (ctepley@naic.edu)
Eva Robles (erobles@naic.edu)

Abstract: This work presents a study about the neutral wind variability over Arecibo (18.35oN, 66.75oW) using ground-based Fabry-Perot interferometer data acquired from 1980 to 2006 (24 years of experiments). The analyses are to both components of the neutral winds (meridional and zonal) during geomagnetically quiet conditions. The dependence of the winds relationed to the solar variability and seasonality will be showed in this work. A numerical model was developed from the analysis procedures and by the residual of the model results and Fabry Perot Interferometer Data the long trend variation will be analyzed.

MLT-04 A Detailed Error Analysis for Meteor Radar Systems - by Chunmei Kang

Status of First Author: Student IN poster competition PhD

Authors: Chunmei Kang, chunmei.kang@colorado.edu, Aerospace Engineering Science, University of Colorado, Boulder, Scott Palo, scott.palo@colorado.edu, Aerospace Engineering Science, University of Colorado, Boulder.

Abstract: Meteor wind radar systems are typically designed to study the horizontal wind field in the mesosphere and lower thermosphere (MLT). While such systems have operated for many years, a comprehensive error analysis is not available in the literature. In this work a detailed analysis of the uncertainty for the parameters derived from meteor radar measurements is presented. The parameters of interest include range, diffusion coefficient, Doppler shift, and angle of arrival (AOA), among which

the range uncertainty is completely determined by the radar sampling rate and can be very precise, e.g. 333.3KHz sampling rate corresponds to 450m uncertainty. Uncertainties of diffusion coefficient, Doppler shift and AOA are demonstrated to be sensitive to the signal-to-noise ratio (SNR) and the true value of the diffusion coefficient. Echoes with high SNR and small diffusion coefficient always have higher precision. Additionally, the AOA measurements are also a function of the angles themselves and the configuration of the interferometer that is used to measure the AOA. High elevation angle echoes have smaller uncertainties than low elevation ones.

Based on this analysis a 10dB SNR threshold is suggested for echo processing and error analysis, since the parameters estimated for echoes above this threshold are unbiased for most parameter estimation algorithms. The uncertainties of any unknown parameters can be completely determined by the Cramer-Rao bound (CRB), which is the minimum mean-square-error (MSE) which any unbiased estimator can achieve.

In this work, the CRB of the diffusion coefficient, Doppler shift and AOA are derived. Based on these measurements, the horizontal wind velocity and the height of the echoes can be determined. The errors in the measurements of the diffusion coefficient, Doppler shift and AOA propagate through the calculations to form the uncertainty of the derived parameters. The horizontal wind velocity is computed by neglecting the vertical component of the vector wind field, which is believed to be more than 10 times smaller than the horizontal wind in amplitude. While the vertical fluctuation is small, neglecting this component increases the bias of the derived horizontal wind especially at high elevation angles, and it becomes the dominant error source above 50 degrees elevation. Below 50 degrees elevation the uncertainty of the horizontal wind velocity is dominated by the uncertainty of the measured radial velocity. The uncertainty is demonstrated to be invariant to the magnitude of the actual wind velocity and minimum uncertainties occur between 30-50 (degree) elevation angles. The height uncertainty decreases as the elevation angle of the echo increases, for a fixed SNR and height, and the height uncertainty at 40(degree) elevation is about 0.5km, however at 30 (degrees) it is increases to 1km.

These results provide more confidence in the meter radar derived parameters and a better understanding of the statistical characteristics associated with meteor echoes. Additionally, the analysis also provides a tool for radar system optimization. For example, if directive transmitting antennas are used, such as the COBRA meteor radar system, an antenna beam elevation of 40 degrees will provide more precise measurements than at the current elevation of 30 degrees.

MLT-05 Deactivation of Highly Vibrationally Excited OH by O Atoms - by Konstantinos Kalogerakis

Status of First Author: Non-student

Authors: K. S. Kalogerakis [1], Gregory P. Smith [1], M. G. Mlynczak [2], and R. A. Copeland [1]
[1] Molecular Physics Laboratory, SRI International, [2] NASA Langley Research Center

Abstract: The hydroxyl radical is a key player in the chemistry and energetics of the middle terrestrial atmosphere, and several studies have investigated energy transfer processes between OH(v) and atmospheric molecules. Nevertheless, a gap exists in our understanding of its interaction with oxygen atoms. Oxygen atoms are present at about 10% of the oxygen molecule concentration at ~95 km and about 1% at 88 km, so if their rate constant is significantly faster than that of O2 and N2, they will strongly influence the intensity and the vibrational distribution extracted from the OH(v) emission.
We report laboratory measurements of the total removal rate constants of highly vibrationally excited OH(v) by O(3P) atoms. These measurements are required so that we can quantify the importance of these collisional processes in the modeling of atmospheric OH emissions and evaluate the chemical heating rate from measurements by the SABER instrument aboard the TIMED satellite.

In the experiments, we generate O(3P) and OH(v) by photodissociation of ozone at 250 nm in a mixture of ozone, nitrogen, hydrogen. We monitor the temporal evolution of the OH(v) population by laser induced fluorescence. By controlling the initial conditions of the experiments, we can extract the rate coefficient for OH(v) removal by O atoms in the system. We will present our results and discuss their atmospheric implications.

This work was supported by the NASA Geospace Sciences and Planetary Atmospheres Programs.

MLT-06 Mesospheric Joule Heating during the Halloween 2003 SuperStorm - by Laura Brower

Status of First Author: Student IN poster competition Masters

Authors: Laura Brower, Jeffrey Thayer, Gang Lu

Abstract: During the intense geomagnetic storm of Oct 28-30, 2003, resulting from the large solar flare/coronal mass ejection (CME) event, high-latitude D-region electron densities were detected by the Sondrestrom incoherent scatter radar (ISR) and reached levels comparable to, and in excess of, typical sunlit E-region densities. The observed D-region electron density between 65 and 95 km indicates discrete enhancements associated with relativistic electron precipitation and diffuse enhancements due to proton precipitation. The diffuse D-region electron density remained in excess of 1011 m-3 throughout the four hour radar observing period with very little fluctuation over that time period . In addition, electric fields exceeding 80 mV/m are detected by the radar. The combination of large electric fields and enhanced D-region density leads to significant electron frictional heating. Based on observed electron densities, an 80 mV/m electric field can cause up to 4 K/day direct heating to the neutral gas; these rates rival other energy sources for the D-region. Modeling efforts typically assume all electron energy contributes to direct heating of the neutral gas Thus, electron frictional heating can be an important contributor to the energy balance of the mesosphere during solar proton/CME events. We will present the Sondrestrom radar observations and model simulations by the NCAR TIME-GCM to study the processes at play. In addition, it has been established by spacecraft and ground-based observations for this event, that the proton flux and electric field enhancements extend over most of the polar cap. Thus, the detailed observations and analysis presented here can be considered to affect a more extensive area of the high-latitude D-region / mesosphere.

MLT-07 Simultaneous Observation of Gravity Waves in Temperature by Using Rayleigh Lidar and Sodium Lidar - by Xian Lu

Status of First Author: Student NOT in poster competition PhD

Authors: Xian Lu, Alan Z. Liu, Gary Swenson, Tao Li

Abstract: Atmospheric gravity waves (GW) play important roles in transporting energy and momentum, in influencing the mean circulation, thermal structure and variability of the middle atmosphere. Observation of the gravity wave characteristics such as wave scales, amplitudes, spectra are essential to understand their momentum fluxes, instability dynamics, seasonal and geographic variability, etc. However, due to their wide range of temporal and spatial scales, observations of GWs are still very limited comparing to their almost ubiquitous existence in the atmosphere. Lidars can carry out observations from the troposphere up to the lower thermosphere with decent time and height resolutions, providing a favorable method to study the spectra, spatial scale and vertical propagation of gravity waves.

In this work, we use the temperature measured by a resonance sodium wind/temperature lidar at Maui (20.7oN, 156.3oW, 84 - 103km) and by a Rayleigh temperature Lidar at Mauna Loa (19.5oN, 155.6oW, 35 - 80 km) on the night of Oct 28, 2003, to study gravity wave activities from the lower stratosphere up to the mesopause region. Nightly mean and fluctuations of temperatures are derived and dominating vertical wavelengths are determined to be ~ 9.6 km for both lidar measurements. Waves seem to be dissipated at the height of 55-65 km which is a less stable atmosphere layer with smaller positive buoyancy frequencies. Wave amplitudes in terms of relative temperature perturbations are derived for lower (35 - 55km) and upper (84 - 103km) layers separately. It shows that the amplitudes at upper layer are 2-4 times larger than at the lower layer, which suggests that the 9.6 km-GWs can propagate upward even after experiencing some dissipation in the middle layer (55 - 65 km). Wave periods are found to be ~ 9.0 hours at the upper layer and ~10.7 hours at the lower layer, indicating a low-frequency GWs.

MLT-08 Simulated ducting of high-frequency atmospheric gravity waves in the presence of background winds - by Yonghui Yu

Status of First Author: Student NOT in poster competition PhD

Authors: Yonghui Yu (1, 2) and Michael P. Hickey (1, 2)
(1) Department of Physical Sciences, Embry-Riddle Aeronautical University, Daytona Beach, Florida, USA
(2) Department of Physics, University of Central Florida, Orlando, Florida, USA.
Michael.Hickey@erau.edu; Yonghui.Yu@erau.edu

Abstract: A new nonlinear and time-dependent model is used to derive the total perturbation energy flux of two gravity wave packets propagating from the troposphere to the lower thermosphere. They are excited by a heat source and respectively propagate in an eastward and westward direction in the presence of a zonal wind. Analysis of the refractive index, the power spectra and the total perturbation energy flux allows us to correctly interpret the ducting characteristics of these two wave packets. In our study the wind acts as a directional filter to the wave propagations and causes noticeable spectral variations at higher altitudes. We are the first that time-resolve the total perturbation energy flux influenced by the winds and the simulations have immediate impacts to the airglow observations on certain wave spectra.

MLT-09 The Lightning associated sudden brightness at the OH airglow altitude: Optical emissions of N2 1P or OH? - by T.-Y. Huang

Status of First Author: Non-student

Authors: T.-Y. Huang, C. Y. Chiang, C. L. Kuo, A. B. Chen, H. T. Su, and R. R. Hsu, Physics Department, Cheng Kung University, Tainan, Taiwan

Abstract: Observations of TLEs by ISUAL broadband filter onboard FORMOSAT-II have sometimes shown an enhancement accompanied by lightning activity at the OH nightglow altitude. Due to too much overlapping of OH and N2 spectrum within the bandwidth of the broadband filter, it was not possible to determine whether the enhancements were elves or lightning induced sudden OH brightness. Simulations of the spectrum of elves (Kuo et al., 2006) reveal that the intensity of N2 1P is very small at 630 nm. The simulations of sprite-induced OH nightglow emission (Huang, 2006) have shown that the column-integrated OH intensity could be enhanced quite significantly when lightning occurs. In response to the need to understand the causes for such enhancements, ISUAL conducted a 9-day campaign in January 2007, with some observations devoted exclusively to capturing TLEs with the 630 nm filter for such an investigation. We will present the analysis of the observations from the CCD camera and spectrophotometer, and will discuss the implications of the results.

MLT-10 Characterization of stratospheric gravity waves by lidar in Antarctica - by Chihoko Yamashita

Status of First Author: Student IN poster competition PhD

Authors: Chihoko Yamashita1, Xinzhao Chu1, Wentao Huang1, Graeme Nott2, Patrick Espy3
1 Department of Aerospace Engineering Science, University of Colorado at Boulder, USA
2 Department of Physics and Atmospheric Science, Dalhousie University, Halifax, Canada
3 Physical Sciences Division, British Antarctic Survey, Cambridge, UK

Abstract: Gravity waves (GWs) play an important role in the dynamics of global middle and upper atmosphere. However, quantitatively characterizing GW in the upper stratosphere is still rare in Antarctica. Here we present a study of stratospheric GWs using the data obtained with the University of Illinois Fe Boltzmann/Rayleigh lidar at the South Pole (90□S) from December 1999 to January 2001 and at Rothera (67.5□S, 68.0□W) from December 2002 to March 2005. The Rayleigh density data in 30-45 km are used to derive GW parameters. Obtained results at South Pole and Rothera are comparable; the observed GW vertical wavelength is ~4.4 km, vertical phase speed is ~0.33m/s, and the period is ~245 min. The root-mean-square (RMS) relative density perturbation is used to characterize the stratospheric GW strength. The seasonal variation of GW strength is clear at Rothera, with maximum in winter and minimum in summer. There is no significant seasonal variation observed at the South Pole. Two important factors, the wind filtering effects and topographical GW source difference, are investigated for the explanation of GW seasonal variations. In addition, abnormal GW strength points are observed in April and September at South Pole. The relations between these abnormal points and the polar vortex formation and breaking are also investigated.

MLT-11 High-Resolution Doppler-Free Spectroscopy for Doppler Lidars - by Wentao Huang

Status of First Author: Non-student

Authors: Wentao Huang1, Xinzhao Chu1, Johannes Wiig1, Paloma Farias1 and Jonathan Friedman2
1Cooperative Institute for Research in Environmental Sciences and Department of Aerospace Engineering Sciences, University of Colorado at Boulder, Boulder, Colorado, USA
2NAIC Arecibo Observatory, Arecibo, Puerto Rico

Abstract: Using high-resolution Doppler-free spectroscopy to lock laser frequency to desired atomic absorption lines and to precisely measure isotope shifts is crucial in developing high-accuracy, high-precision, and bias-free Doppler lidars. Although fluorescence spectroscopy is widely used in the current state-of-the-art Na and K Doppler lidars to lock the cw seed lasers to the Na and K Doppler-free features, it suffers low signal-to-noise ratio, dither and chirp problems during pulsed amplification for lidar applications. We investigated the saturation absorption and polarization spectroscopy, which are much sensitive and can apply to the pulsed laser frequency locking directly. This will achieve not only high SNR but also dither-free and chirp-free thus bias-free measurements of key environmental parameters. Here we focused our study first on K, will extend the analysis to Na and Fe later.

Mesosphere or Lower Thermosphere - Lidar

LID-01 Polar Stratospheric Clouds at Rothera (67.5°S, 68.0°W) and South Pole: Lidar Observations and Polar Vortex Effects - by Wentao Huang

Status of First Author: Non-student

Authors: Wentao Huang1, Xinzhao Chu1, Shawn E. Simpson2, Walter Robinson3, Graeme J. Nott4, Patrick J. Espy5
1Cooperative Institute for Research in Environmental Sciences and Department of Aerospace Engineering Sciences, University of Colorado at Boulder, Boulder, Colorado, USA
2Department of Statistics, Columbia University, New York, New York, USA
3Department of Atmospheric Sciences, University of Illinois at Urbana-Champaign, Urbana, Illinois, USA
4Department of Physics and Atmospheric Science, Dalhousie University, Halifax, Nova Scotia, Canada
5Physical Science Division, British Antarctic Survey, Cambridge, UK

Abstract: We report the first groundbased lidar observations of polar stratospheric clouds (PSC) in the West Antarctica. The observations were made with an iron Boltzmann/Rayleigh/Mie lidar at Rothera (67.5°S, 68.0°W) in the austral winters and springs of 2003 and 2004. Rothera observations are compared to those made by the same lidar in 2000 and 2001 at the South Pole (90°S). Overall PSCs are observed in the altitude range of 12-28 km from May/June to September/October at both locations with comparable mean peak backscatter ratio, centroid altitude, and RMS layer width. PSCs occur much less frequently and in shorter period at Rothera than at the South Pole, which is consistent with the longer persistence of lower temperature favorable for PSC formation at the South Pole. Rothera PSC season began later and ended earlier in 2004 than in 2003 due to the warmer temperature in early winter and late spring of 2004. Thus, PSC occurrence correlates well with local temperature at 50 mbar, which is in turn strongly affected by the activity of Antarctic polar vortex. When the vortex edge approaches and crosses Rothera from the south, the local temperature decreases and PSCs usually occur if the temperature drops below 194 K. Unusual cases occur when Rothera is well within the vortex and temperature is below the threshold but no PSCs are observed. They are likely caused by the polar vortex preventing tracer gas (NAT) transportation across the vortex boundary when the stratosphere is denitrified and dehydrated in spring.

LID-02 CRRL/CTC: Web-based Lidar Simulation Tool for Doppler and Rayleigh Lidars - by Paloma Farias Gutierrez

Status of First Author: Student IN poster competition PhD

Authors: Paloma Farias Gutierrez 1, Johannes Wiig 1, Wentao Huang 1, Xinzhao Chu 1, Jonathan Friedman 2
1) Cooperative Institute for Research in Environmental Sciences & Department of Aerospace Engineering Sciences, University of Colorado; 2) NAIC Arecibo Observatory, Arecibo, Puerto Rico

Abstract: The Lidar Consortium Center (CTC) is being built at the University of Colorado at Boulder, under the umbrella of the Consortium of Resonance and Rayleigh Lidars (CRRL). A lidar simulation tool with error analysis for K, Na, and Fe Doppler lidars and Rayleigh lidars will be available at the CRRL/CTC website for public access. The simulation results are compared to lidar data from the Arecibo Observatory. A study of how to extend the simulation for use with daytime measurements is also presented. This new tool facilitates the validation of observations, aids the lidar system design, and helps educate the next generation of lidar users and designers.

LID-03 CRRL/CTC: New suite of DAQ and control system for lidar applications and laser spectroscopy - by Johannes Wiig

Status of First Author: Student IN poster competition PhD

Authors: Johannes Wiig, Paloma Farias Gutierrez, Wentao Huang, and Xinzhao Chu

Abstract: Currently, the lidar Consortium Technology Center (CTC) is developing a new suite of lidar DAQ and control system. It provides a user-friendly interface to control, monitor, and record laser frequency, stabilize vapor cell temperature, acquire lidar data, and optimize lidar beam alignment. This poster illustrates the design, setup, and functionality of the system. Also presented is the saturation-absorption spectroscopy of Na, K, Rb and, Cs obtained with this new suite. This is a first step by CRRL/CTC to unify the control and DAQ approach used by ring-dye based Doppler lidar systems.

LID-04 Maui/MALT Enterprise Lidar Receiver: Urbana observations and performance - by Chad G. Carlson

Status of First Author: Student NOT in poster competition PhD

Authors: C.G. Carlson, G.R. Swenson, A.Z. Liu, T. Mangognia, B. Graf, A. Kirchhoff, and D.S. Anderson
Dept. of Electrical and Computer Engineering, University of Illinois at Urbana-Champaign

Abstract: During the past three years, the Maui/MALT Na wind/temperature lidar system has been moved from Haleakala, Maui, HI to Urbana, IL and updated by a team of students and faculty from the University of Illinois at Urbana-Champaign. Specifically, a new four telescope array receiver with efficient photon detectors, minimal coupling optics, and fast counting electronics has been designed, built, and integrated with the Na wind/temperature lidar transmitter. The design and theoretical performance of the new system will be discussed. Additionally, recent lidar observations of temperature and Na density in the MLT region over Urbana, IL will be presented and the performance of the new receiver will be compared with the previous instrument that used a telescope with 5 times the receiving aperture.

LID-05 Initial progress toward an all-solid-state lidar and OH image observations with Na lidar measurements - by Jia Yue

Status of First Author: Student IN poster competition PhD

Authors: Yue, She, Reising, and Nakamura

Abstract: A single-pass Sum-Frequency-Generation (SFG) with two monolithic YAG CW lasers (at 1064 and 1319 nm) has been constructed, producing 1 mW of tunable CW light at 589 nm. Using Doppler-free fluorescence spectroscopy, the generated yellow light can be locked at the sharpest lamb dip of the Na D2a transition for hours. With the feedback from Doppler-free spectroscopy, the frequency of the YAG laser at 1064 nm is adjusted automatically using a control computer so that the summed frequency with 1319 nm laser stays constant within a range of 1 – 2 MHz. This system will guide the accurate seeding of the transmitter for the proposed high-energy pulsed all-solid-state Na temperature/wind lidar transmitter.

The Kyoto University OH imager at Yucca Ridge Field Station (40.7N, 104.9W) has been observing gravity waves since 2003. Recently, CSU is helping to maintain the instrument for the purpose of collaborative observations with the nearby CSU sodium lidar (40.6N, 105.1W), which observes mesopause-region temperature, zonal and meridional winds over 24-hour periods. Initial examination of the OH images reveals a very active mesopause region, containing propagating mesospheric bores and walls. On the night of Sep. 8, 2005, the imager also observed an unusual, possibly new feature of a revolving "localized" circular wave pattern that lasted the entire night. We hope to continue the investigation of these images and, when feasible, to perform correlative studies with concurrent lidar observations.

LID-06 The MLT metal layer topside: LIDAR observations of micrometeor influx? - by Jonathan S Friedman

Status of First Author: Non-student PhD

Authors: Jonathan S. Friedman, NAIC Arecibo Observatory (jonathan@naic.edu)
Josef Höffner, Leibniz Institute for Atmospheric Physics (hoeffner@iap-kborn.de)

Abstract: The mesosphere and lower thermosphere metal layer is seen to extend well past the 105 km usually quoted as the upper extent. Seasonal and nocturnal characteristics of the layer when multiple metals are observed show that it is very different from the better-known 80-105 km layer. We ask the question: Given its characteristics, if this extension is not directly attributable to micrometeor influx, then what would be the source?

LID-07 The new mobile scanning Fe-Doppler lidar: Spectral measurements of Resonance, Rayleigh and Aerosol scattering from the troposphere to the mesosphere - by Josef Hoeffner

Status of First Author: Non-student

Authors: Hoeffner, J. and J. Lautenbach, Leibniz-Institute of Atmospheric Physics, Germany
Hoeffner@iap-kborn.de

Abstract: First measurements of Doppler temperatures and winds at the iron resonance line at 386 nm in 2002 have shown that a mobile scanning Fe-Doppler lidar has many advantages about nowadays doppler lidar. Nearly background free measurements at daylight should be possible due to the favourable combination of low backscatter coefficient and large iron number densities if efficient narrowband spectral filtering and small field of views (FOV) can be achieved.

Starting in 2004 we have converted the former containerized K-lidar to a mobile Fe-lidar. After first successful daylight measurements in 2005 with a single etalon and a FOV of 0.05 mrad we have achieved nearly background free measurements in 2006 with a 2 pm FWHM double etalon.

The main challenge for Doppler measurements is the precise determination of the spectral filtering in the receiver which influences the intensity measurement. The spectral filtering of an etalon depends on the properties of the incoming beam and alignment and environment and can therefore not be measured in advance in the laboratory with high precision. The Fe-lidar determinates the filter functions of the double etalon during each measurement from the atmospheric measurements itself.

After successful simultaneous measurements at two wavelengths we have extended the lidar by adding a similar double etalon at 772 nm with a FWHM below the Doppler width of Rayleigh scattering (~1200 MHz). The observed spectrum allows to distinguishing between Aerosol and Rayleigh scattering. Measurements at stratospheric heights show that it is possible to measure the Aerosol contribution first, correct the backscattered signal for this contribution and finally calculating Rayleigh temperatures from the corrected signal. Additionally Doppler temperature and wind can be calculated from the Rayleigh signal. Even though the 772 nm double etalon can not benefit from a Fraunhofer line we have achieved also nearly background free daylight measurements with this technique.

With an additional confocal etalon locked to an atomic reference spectral filtering in the order of the line width of the pulsed laser is now possible. Beside background free Doppler measurements of Aerosols this technique reduces the contribution from Rayleigh scattering roughly 100 times. With a commercial 2 MHz FWHM confocal etalon we have measured Doppler winds with uncertainties in the order of a few cm/s at the troposphere and lower stratosphere. An optimized design with ~100 times improved performance is under development and will extend these measurements to mesospheric altitudes.

Currently the scanning Fe-lidar is a two wavelength system with 8 channels and 5 Etalons. All observed quantities such as laser power, count rate profile or laser spectrum and frequency of the pulsed laser are measured pulse by pulse and stored on disk with 25 m resolution. The laser system can be programmed between two laser pulses to any frequency with ~10 MHz precision in a frequency range of ~10.000 MHz. The precise frequency is measured after each laser pulse with sub-MHz resolution. This approach overcomes common problems of frequency shifts between seeder lasers and pulsed lasers. Similar to the former K-lidar the Fe-lidar needs no atomic reference at the observed wavelength and this technique can therefore be overtaken to any wavelength in the range of the laser with similar performance.

Yee Posters: MLT Climatology

YEE-01 Seasonal variations of semidiurnal tidal-period perturbations in mesopause region temperature, zonal and meridional winds above Fort Collins, CO (40.6°N, 105°W) - by Tao Yuan

Status of First Author: Non-student PhD

Authors: Tao Yuan, C. Y. She, David A. Krueger, Department of Physics, Colorado State University, Fort Collins, CO 80523
Hauke Schmidt, Max Planck Institute for Meteorology, Hamburg, Germany
titus@lamar.colostate.edu,,joeshe@lamar.colostate.edu, krueger@lamar.colostate.edu, hauke.schmidt@zmaw.de

Abstract: Based on Colorado State University Na lidar observation (May 2002 - April 2006) over full diurnal cycles, harmonic analysis was performed to extract semidiurnal perturbations in mesopause region temperature, zonal and meridional winds over Fort Collins, CO (40.6N, 105W). We compared the lidar results to the 3-year Hamburg Model of the Neutral and Ionized Atmosphere (HAMMONIA), binned in 3-hour. The model prediction agrees very well with lidar observations. We found the semidiurnal tide over mid-latitude at mesopause reigon is dominated by propagating mode with the vertical wave length varying from 50 km to almost 90 km. The semidiurnal tidal amplitude shows strong seasonal variation with its peak amplitude during the winter months and its minimum during the summer, which is consistent with classical tidal theory. However, the considerably large tidal amplitude during equinox, along with the complex tidal behavior during summer, revealed in both model prediction and observation is puzzling. In addition to monthly semidiurnal tides, we use simplified linear tidal theory equations to compute the vertical wavenumber of the dominant semidiurnal tidal modes based on CSU Na-lidar mean temperature and zonal wind climatology of the mesopause region at mid-latitude. The results show that the vertical wavenumber seasonal variation is accompanied with the tidal amplitude increase during equinoxes, possibly resulting from refractive effects on the semidiurnal tidal waves. The summer complex tidal behavior could be due to the dissipation that ceases the exponential growth of the tidal amplitude.

YEE-02 An analysis of mid-latitude neutral wind in the lower thermosphere: comparison of fall and spring equinoxes - by Larisa Goncharenko

Status of First Author: Non-student

Authors: Goncharenko L. P., K. Reed, A. Mazurkar

Abstract: We present an analysis of tidal structures in the altitude range of 100 to 130 km for the September 1-30, 2005 and March 6-April 6, 2006 periods using the winds measured by the Millstone Hill incoherent scatter radar. The dominant signal in both zonal and meridional winds is the semidiurnal component, as expected from the tidal theory and previous experimental data. Both zonal and meridional components of semidiurnal tide are stronger during spring equinox, reaching 70-80 m/s, and have a well defined maximum around 110-118 km. In September, amplitude of 12-h tide peaks at ~112km and 60-65 m/s for the meridional component, while the zonal component exceeds 50 m/s in range of altitudes from 105 to 130 km. The diurnal tide, which has often been assumed negligible in earlier observations, is found at altitudes ~105-120 km. It is stronger in September, reaching ~15-20 m/s, and is under 10 m/s in March. The phase structure of the diurnal tide indicates domination of the in-situ generated tide. The background wind is mostly northward for the meridional component, with well pronounced altitude gradient, and westward for the zonal component.

YEE-03 Spectral Characteristics of Neutral Wind in the Lower Thermosphere at Middle Latitudes: Comparison of September 2005 and March 2006 Data - by Amrita Vijay Masurkar

Status of First Author: Student IN poster competition Undergraduate

Authors: Amrita Masurkar, spamrita@mit.edu, Larisa Goncharenko, lpg@haystack.mit.edu

Abstract: Neutral wind data obtained with the Millstone Hill Incoherent Scatter Radar during the September 2005 and March 2006 campaigns were spectrally analyzed and compared. Lomb-Scargle (LS) analysis was performed on the month-long time series, and a Fast Fourier Transform was used on one-day segments and monthly averages for the purpose of detecting periods on the order of a few hours. LS periodograms for both campaigns indicate the presence of 8-hr, 12-hr, 24-hr, quasi-two-day and quasi-five-day waves in the meridional and zonal components. Although averaged data from both campaigns does not provide

strong evidence of a terdiurnal wave, an 8-hr component appears in one-day segments more frequently in September than in March. In addition, testing for spectral leakage shows that significant contributions to the 8-hr component are made from interactions between the 12- and 24-hr peaks and harmonics arising from nighttime data gaps.

Polar MLT Aeronomy

POM-01 High altitude Interferometer WIND observation (HIWIND) - by Qian Wu

Status of First Author: Non-student

Authors: Qian Wu

Abstract: We propose to build a balloon-borne Fabry-Perot Interferometer to observe the thermospheric neutral wind over the northern polar cap by launch balloon from Kiruna, Sweden. Polar cap thermosphere is strongly affected by the magnetosphere through ionosphere-thermosphere interaction. The thermosphere neutrals are dragged by the ions, which are driven by the cross-polar cap potential. The cross-polar potential is a direct result of the solar wind dynamos. The ion and neutral collision is an energy transfer process from ionosphere to the thermosphere. Part of the energy is transformed to the neutral kinetic energy with an increase of the neutral wind speed, other part of the energy is converted to the heat through Joule heating. Joule heating raises the thermosphere temperature and causes upwelling and changes thermosphere composition and ion density. The high latitude ionosphere thermosphere interaction has a great impact on the global thermosphere circulation and is of great interest to space weather and ionosphere magnetosphere study. To achieve a better understanding of ionosphere thermosphere interaction, we must know the thermosphere winds in order to precisely estimate the Joule heating. Currently, only ground based Fabry-Perot interferometers are able to measure the thermosphere neutral winds during nighttime by monitoring O 630.0 nm nightglow from 250 km altitude. Daytime ground based Fabry-Perot measurements of thermosphere neutral winds have large uncertainties due to the high background from the scattering of sunlight. That means most of observations are limited to the northern winter season. There are several high latitude incoherent scatter radars (EISCAT, Sondrestrom, and AMISR), which can provide ion drift data day and night. During the northern summer season, when the northern polar region is under constant daylight, we do not have any thermospheric neutral wind coverage. The ionosphere density is different during winter and summer; hence the interaction between the ionosphere and thermosphere is also different. Currently there are no satellite observations of the thermospheric wind. The proposed balloon borne Fabry-Perot interferometer will be able to fill in this critical data gap by providing the much needed summer day time polar cap thermospheric neutral wind data. A balloon Fabry-Perot interferometer is not affected by the scattering of the sunlight, when it flies at stratosphere heights. We intend to coordinate the future balloon flights with ground based radar operation from EISCAT, Sondrestorm, to AMISR, which will be on the flight path. If the project is successful, we intend to fly the instrument at other latitudes where the day time thermospheric neutral winds are also in great demand. We envision use this instrument to validate the future CINDI instruments on C/NOFS satellite.

POM-02 Time Evolution Imaging of Polar Mesospheric Clouds Using Airborne and Spaceborne Platforms - by Jason Reimuller

Status of First Author: Student IN poster competition PhD

Authors: Jason D. Reimuller, Jeffrey P. Thayer, Stephen Corda, Aimee Merkel, and Mike Taylor

Abstract: Polar mesospheric clouds (PMCs) are the focus of NASA's Aeronomy of Ice in the Mesosphere (AIM) satellite, launched in April 2007. A unique opportunity arises to study PMC structure and temporal development by performing airborne PMC observations and coordinating them with AIM overpasses. The proposed research builds on a 30-day aircraft flight experiment to be carried out in July/August 2007 in Alaska consisting of IR and near-UV optical sensors to image PMCs over several hours. The complementary nature of airborne measurements, continuously imaging PMCs, and satellite measurements, providing extensive polar coverage, would enable the first detailed study of the temporal evolution in PMCs. The synchronous aircraft and satellite images will also provide deeper understanding of the PMCs scattering properties. By better understanding PMCs, we hope to gain insight into 1) the elements of global climate change believed to cause their expanding presence, 2) high-altitude, low-density clouds on other worlds, and 3) mesospheric science and the potential risk PMCs pose to reentry vehicles.

POM-03 Polar Mesospheric Summer Echoes (PMSE) overshoot effect - Theory and Observations - by Chen Chen

Status of First Author: Student IN poster competition

Authors: Chen Chen & Wayne Scales, Virginia Tech, chenc@vt.edu, wscales@vt.edu

Abstract: Polar Mesospheric Summer Echoes (PMSEs) are strong radar echoes from electron irregularities of meter scale or less in the earth's mesosphere. The electron irregularities believed to produce PMSEs result from electron charging on subvisible dust that exists in the mesosphere. The dust is primary ice particles since the summer polar mesosphere is the coldest region in the earth's atmosphere. Previous experimental observations have shown that PMSE may be modulated by radio wave heating the irregularity source region with a ground-based ionospheric heating facility. It is clear from past investigations that the temporal behavior of PMSE during ionospheric heating shows promise as a diagnostic for the associated dust layer. Previous works used both discrete and continuous charging models to investigate temporal behavior of electron irregularities during electron temperature enhancement associated with radio wave heating. The models utilize fluid ions described by continuity and momentum equations, electrons whose behavior is determined from quasineutrality, and charged dust described by the standard Particle-In-Cell PIC method. The results of both the continuous and discrete models show that the temporal behavior of the irregularities depends on the ratio of the electron-ion ambipolar diffusion time to the dust particle charging time Tdiff/Tchg. The results indicate that typically for Tdiff/Tchg<<1, , an overshoot occurs during turn-off of the radio wave heating. This is the regime of previous models which incorporated Boltzmann electrons. The work also predicts that for Tdiff/Tchg>>1, a turn-on overshoot should be observed in which there is an increase in PMSE amplitude for a short period of time before ultimate suppression of the PMSE during continued heating. Also, for sufficiently large Tdiff/Tchg, the PMSE amplitude may be enhanced during the entire heating period. Due to the dependence of Tdiff on irregularity scale-size, these results have important implications for observations of PMSE modification at different radar frequencies. The August, 2006 campaign in HAARP, Alaska used 4.9 MHz radar for the PMSE turn-on overshoot observation. Experiment results showed the enhancement of radar backscatter signal power during the PMSE heating. More experiments must be done to test the validity of the turn-on overshoot effects and before definitive conclusions can be drawn.

POM-04 PMSE MST Radar Statistics From Antarctic Peruvian Station - by Henry Pinedo Nava

Status of First Author: Student IN poster competition Masters

Authors: H. Pinedo(1), L. Flores(2), R. Woodman(1) and J. Chau(1)
(1) Instituto Geofísico del Perú – Jicamarca Radio Observatory, Apartado 13-0207, Lima 13, PERU
(2) Universidad de Piura – Laboratorio de Física y Meteorología, Apartado 353, Piura, PERU

Abstract: The MST radar facility located at the Machu-Picchu Peruvian Station in Antarctica (62º,06' S, 58º28' W), was used by the Peruvian Atmospheric Research Group in 1994 to make the first Polar Mesosphere Summer Echoes (PMSE) measurements in the Southern Hemisphere. Previous campaigns which have been published in the literature (Balsley et al. 1995, Woodman et al. 1999) and reported at MST conferences (Sarango et al. 2003) have concluded the following: there exists an (Arctic-Antarctic) inter-hemispheric asymmetry in PMSE intensity and there exists an inter-annual variability in the scattering phenomena. Motivated by these findings, a new VHF radar was installed at the Machu-Picchu station in December 2006. This new array consisted of three Yagi sub-arrays (15m x 15m each) and the same number of receiver channels allowing the calculation of wind speeds using spaced antenna techniques. In this presentation we analyze the data from the Machu-Picchu 2006-2007 campaign, and then compare the results with Artigas 2000-2001 (62º11' S, 58º54' W) and Machu-Picchu 1997-1998 campaigns. The Artigas and Machu-Picchu stations are located approximately 30km apart on King George Island. We show the seasonal and diurnal SNR and occurrence maps for the entire campaign (and projections on axes), the maximum power level map and a graph of the occurrence ratio versus PMSE minimum level threshold.

POM-05 Gravity wave observations from Rayleigh scatter measurements: A comparison of OMI data variability with CIPS simulations - by Amal Chandran

Status of First Author: Student IN poster competition PhD

Authors: Amal Chandran1, David Rusch2, Cora Randall2, Scott Palo1
1Department of Aerospace Engineering, University of Colorado, Boulder

2Laborotary for Atmospheric and Space Physics, University of Colorado, Boulder

Abstract: Wave structures observed in the Rayleigh scatter measurements from the Ozone Monitoring Instrument (OMI) on board the NASA AURA satellite are compared with gravity wave simulations run for the Cloud Imaging and Particle Size (CIPS) instrument. Omi is a nadir pointing imaging spectrograph that measures solar radiation in the UV and visible spectral range between 270 and 500 nm. Wave structures with horizontal wavelengths extending up to 2000 kilometers and spread over 25 degrees in latitude in the Northern hemisphere can be observed from plots of the difference between the observed Rayleigh scatter measurements and a smooth polynomial fit to the measurements. CIPS measures primary scattering from Polar Mesospheric Cloud's (PMC) near 82 km altitude and also additional Rayleigh scattering near 50 km altitude that may indicate gravity wave activity. CIPS simulations were run with gravity waves of different wavelengths perturbing the ozone background and compared with the OMI data variability.

POM-06 Comparison of Satellite and Ground-Based Data on Polar Mesospheric Clouds - by Jodie Barker-Tvedtnes

Status of First Author: Student IN poster competition Undergraduate

Authors: Jodie Barker (Utah State University) , Mike Taylor (Utah State University) , Matt Deland (Science Systems and Applications Inc., Maryland), Mark Zalcik (Edmonton, Canada)

Abstract: In preparation for coordinated ground-based optical measurements with the recently launched NASA Aeronomy of Ice in the Mesopause (AIM) satellite we have examined data mainly from the Solar Backscatter Ultraviolet (SBUV) instruments onboard the NOAA polar orbiting satellites. Our primary goal is to investigate the detection of Polar Mesospheric Clouds (PMCs) over the North American continent using data over five consecutive years (2001-2005). PMCs are ice clouds that form near the extremely cold (<150K) mesopause region (80-85 km) during the summer months at high-latitudes. From the ground, these clouds can be seen during twilight hours as Noctilucent or "night shinning" Clouds (NLC). In particular, SBUV satellite observations have shown that the occurrence and brightness of PMCs have been growing over the last several decades prompting speculation concerning their role in climate change. In this poster we compare reports of displays seen from the ground over the North American continent primarily by observers participating in the Canadian Noctilucent Cloud Observing Network CAN AM with the SBUV as well as new Ozone Monitering Instrument (OMI) satellite data. Our focus is to investigate the occurrence and spatial extent of the clouds, as well as to identify unusual low latitude events (<50 deg) that have occasionally been seen as far south as Logan, Utah.

POM-07 Arctic Wintertime Mesospheric Coolings and Stratopause Warmings - by Katelynn Greer

Status of First Author: Student IN poster competition Undergraduate

Authors: Katelynn Greer (University of Colorado), Jeffrey P. Thayer (University of Colorado), John Livingston (SRI International), and Abas Sivjee (Embry-Riddle Aeronautical University)

Abstract: The arctic mesosphere experiences temperature decreases of ten's of kelvins during the winter. Correspondingly stratopause temperatures increase by ten's of kelvins during the mesospheric cooling events. We investigate the connection between these two phenomena and describe their morphology.

POM-08 The Tristatic Alaskan Fabry-Perot Interferometer Network - by Russell Hedden

Status of First Author: Student IN poster competition Undergraduate

Authors: Russell Hedden, John Meriwether, Michael Faivre, Miguel Larsen, Don Hampton

Abstract: An important issue in polar studies of thermospheric dynamics is the question of ion-neutral coupling by which plasma convection transfers momentum to the background neutral atmosphere. A new Fabry-Perot observatory network has been established in central Alaska at the three sites of Poker (65.117 N, 147.143 W), Fort Yukon (66.568 N, 145.256 W), and Eagle (64.786 N, 141.200 W) that observes the Doppler shift and Doppler width of the 630-nm airglow or auroral emisson. The initial results from the 2007 winter season are presented.

POM-09 An investigation on atmospheric characteristics and the height of airglow emissions inferred from SATI and VHF meteor radar instruments at King Sejong Station (62 S, 58 W), Antarctica - by Jeong-Han Kim

Status of First Author: Student IN poster competition PhD

Authors: J.-H. Kim, C. S. Lee, Y. H. Kim, G.H. Jee

Abstract: We have been operating a SATI instrument for observation of O2(0-1) and OH(6-2) airglows since 2002 and a VHF meteor radar since March 2007 at King Sejong Station(62 S, 58 W), Antarctica. The meteor radar can measure numerous meteor trails, and their decay rates provide ambipolar diffusion coefficients at the meteor altitudes. The diffusion coefficient is known to be closely connected to the local atmospheric temperature and density. In this study, we investigate the relations between two rotational temperatures from the SATI and the ambipolar diffusion coefficients from the meteor radar near the peak altitudes of O2(0-1) and OH(6-2) airglows by using southern fall data of March 2007 through June 2007. The results show that the rotational temperatures have a good correlation with the diffusion coefficients near the previously known airglow peak altitudes. We will discuss about the altitudes of both O2(0-1) and OH(6-2) airglows that have a maximum correlation between temperatures and ambipolar diffusion coefficients by comparing our results with other studies. The estimated densities from diffusioni coefficients at the altitudes that have maximum correlations seem inversely proportional to the SATI temperatures, implying adiabatic nature on the airglow layers.

POM-10 High-speed neutral wind in the polar lower thermosphere observed by the ESR - by Takuo T. Tsuda

Status of First Author: Student IN poster competition PhD

Authors: T. T. Tsuda, S. Nozawa, S. Oyama, and R. Fujii, Solar-Terrestrial Environment Laboratory, Nagoya University, Furo-cho, Chikusa-ku, Nagoya 464-8601, Japan; T. Motoba, Graduate School of Environmental Studies, Nagoya University. Furo-cho, Chikusa-ku, Nagoya 464-8601, Japan; Y. Ogawa, National Institute of Polar Research, 9-10, Kaga 1-chome,Itabashi-ku, Tokyo 173-8515, Japan; H. Shinagawa, National Institute of Information and Communications Technology, 4-2-1 Nukui-Kitamachi, Koganei, Tokyo 184-8795 Japan

Abstract: The high-speed neutral wind was observed by the EISCAT Svalbard Radar (ESR) at Longyearbyen (78.2° N, 16.0° E, 75.2° N invariant latitude) on 16 June 2005. From ~1000 to 1300 UT (~1300-1600 MLT), the observed neutral wind velocity was unusually large and its magnitude at 118 km was more than ~500 m s-1. In the F region, during the same period, the convection electric field reached ~100 mV m-1 under southward IMF conditions (from 0 nT to -15 nT). These results imply that the high-speed neutral wind in the polar lower thermosphere was produced by the strong ionospheric convection due to the southward IMF. However, the estimated ion drag accelerations were insufficient to produce the high-speed neutral wind and thus the acceleration mechanism, which produced high-speed neutral wind, was still unclear. In order to understand the acceleration mechanism for the high-speed neutral wind in more detail, we have analyzed the data of 111 days obtained with the ESR from 1998 to 2005 and selected ten high-speed neutral wind events. Thus, it is considered that the high-speed neutral wind event is, to some degree, rare event. In this paper, we will show the high-speed neutral wind event on 16 June 2005 and discuss the convection electric field and IMF conditions for the high-speed neutral wind using the accumulated ten events.

Mesosphere and Lower Thermosphere - Tidal or Planetary Waves

TID-01 Eastward Propagating Two-Day Waves Observed in the High Latitude Mesosphere and Lower Thermosphere (MLT) - by Joseph Bean

Status of First Author: Student IN poster competition Masters

Authors: Joseph Bean, Loren Chang, Xiaoli Zhang, Scott Palo, Jeffrey Forbes, University of Colorado at Boulder

Abstract: Observational and modeling studies have shown the presence of eastward propagating waves with periods near two-days in the high latitude MLT during winter. These disturbances are believed to be excited by an instability in the westerly zonal mean zonal wind jet, which dominates the middle atmosphere during winter. It has been proposed that wave activity resulting from

this instability can provide local forcing over a range of planetary wave periods and zonal wavenumbers with phase speeds equal to the zonal mean zonal wind speed in the unstable region.

In this study, we analyze ground-based radar data from the South Pole and TIMED SABER temperature observations for signs of these instability driven waves. The TIMED SABER temperature measurements provide information about the spatial structure and zonal wavenumber of the disturbances up to a latitude of 83oN while the South Pole meteor radar observations provide information about the horizontal wind field in the vicinity of the pole. Results from the Whole Atmosphere Community Climate Model (WACCM3) will be used to connect the wind and temperature observations and provide a global context for the generation and evolution of the observed eastward propagating two-day wave.

TID-02 Planetary wave induced migrating diurnal tidal variability in WACCM3 - by Loren Chang

Status of First Author: Student IN poster competition PhD

Authors: Loren Chang, changlc@colorado.edu, Department of Aerospace Engineering Sciences, University of Colorado, Boulder.
Scott Palo, scott.palo@colorado.edu, Department of Aerospace Engineering Sciences, University of Colorado, Boulder.
Jadwiga Richter, jrichter@ucar.edu, Climate and Global Dynamics Division, National Center for Atmospheric Research.

Abstract: While the long term changes in the migrating diurnal tide are related primarily to seasonal variations in the solar heating profile and zonal mean zonal winds, short term variations of the tide on time scales of days to weeks are not well understood. Past studies have suggested that short-term tidal variability can be induced through nonlinear interactions with low frequency and stationary planetary waves, with the former resulting in tidal amplitude modulation with periods close to those of the interacting planetary wave, and the latter resulting in energy transfer to various nonmigrating components of the diurnal tide. In this study, output from version 3 of the NCAR Whole Atmosphere Community Climate Model (WACCM3) is analyzed around the solstices to identify possible migrating diurnal tide / planetary wave interactions, as well as other possible factors which may contribute to short term tidal variability.

TID-03 A Numerical Model for VHF Meteor Radars - by Kyle M Johnson

Status of First Author: Student IN poster competition Masters

Authors: Kyle Johnson - University of Colorado, Dr. Scott Palo - University of Colorado

Abstract: A numerical model is being created that will simulate VHF radar systems designed to detect meteor trails in the upper atmosphere. This model will be used to optimize the system parameters and configuration with respect to key metrics. It will also be used to determine the sensitivity of the system performance to design parameters, to determine the effect of error sources on the estimated wind measurements, and to guide the design of a bistatic or multistatic system. The placement of the transmitter and receivers and the antenna configuration have a large impact on the number of detections and the signal to noise ratio of the reflected signals. It is shown that this VHF radar model can be used to guide the placement of remote receivers. Also, it is shown that this placement is critical to the success of the system and highly dependent on the meteor distribution model.

TID-04 New results on the midnight temperature maximum at equatorial latitudes - by John Meriwether

Status of First Author: Non-student

Authors: J. Meriwether, M. Faivre, C.Fesen, Department of Physics and Chemistry, Clemson University (meriwej@clemson.edu)
O. Veliz, Jicamarca Radio Observatory, Jicamarca, Peru

Abstract: The Arequipa FPI observatory upgraded with a high quality CCD detector observe thermopsheric winds and temperatures with accuracies of 7-8 m/s and 20-25 K for integration periods of 120 s and source signal of 50 Rayleighs. A new observing strategy of 8 equally-spaced azimuths at 60 degrees zenith angle produces data that can be analyzed to produce maps of the neutral wind field and temperature. These results show that when there is no nighttime meridional wind flow the midnight temperature maximum (MTM) is not evident. However, when there is such flow equatorward, the MTM is seen often with an amplitude of 150-200 K. The heating is localized to a region of 300-500 km. The MTM is also seen to progress from the northwest to the southeast of ~300 m/s. Calculations with the NCAR TIME-GCM model do not show such structure even when the terdiurnal forcing has been included as part of the lower boundary. In summary, the MTM is a superb example of the ion-neutral coupling that exists at low latitudes.

TID-05 Investigation of short-period ripple-type wave structures in OH and O2 airglow emissions and associated instabilities in mesopause region over Maui, Hawaii - by Deepak B. Simkhada

Status of First Author: Student IN poster competition PhD

Authors: Deepak B. Simkhada, Utah State University, Center for Atmospheric and Space Sciences and Physics Department 4415 Old Main Hill Logan, UT 84322-4415 dbsimkhada@cc.usu.edu; Michael J. Taylor, Utah State University, Center for Atmospheric and Space Sciences and Physics Department, 4415 Old Main Hill, Logan, UT 84322,mtaylor@cc.usu.edu
Alan Z. Liu, Department of Electrical and Computer Engineering, University of Illinois at Urbana-Champaign 308 Coordinated Sciences Laboratory, 1308 West Main, Urbana, IL 61801, liuzr@uiuc.edu

Abstract: Small-scale ripple structures, which are believed to be manifestations of instability features generated in situ, have been investigated in the mesopause region from Haleakala, Maui, Hawaii (20.70 N, 156.30 W) during the Maui-MALT campaign. The Utah State University Mesospheric Temperature Mapper (MTM) was utilized to sequentially observe ripple events in both the OH and O2 airglow layers centered at ~ 87 km and ~ 94 km respectively, exhibiting horizontal wavelengths of ~ 6-15 km, observed periods of ~ 5-10 min and lifetimes of ~ 15-40 min. In this paper, we have analyzed the nature of the ripple events observed on several nights during 2002-2005 periods, together with measurements of atmospheric winds and instability using co-located University of Illinois Na wind/temperature lidar data. A total 17 ripple events in OH emission and 19 ripple events in O2 emission were observed on 13 nights. Our analyses of these events support recent previous studies that ripples are signatures of local dynamic instabilities which arise from transient large wind shears and large negative vertical temperature gradients.

Mesosphere and Lower Thermosphere - Gravity Waves

GWM-01 An Investigation of the Occurrence of Mesospheric Bores over Bear Lake Observatory, Utah (41.6°N) - by Amauri Fragoso de Medeiros

Status of First Author: Non-student PhD

Authors: A. F. Medeiros1,2, M. J. Taylor2, J. Fechine3, H. Takahashi3, R. A. Buriti1
1 - Universidade Federal de Campina Grande, Brazil,
2 - Center for Atmospheric and Space Sciences, Utah State University, UT, USA
3- Instituto Nacional de Pesquisas Espaciais (INPE), Brazil,

Abstract: All-sky measurements of mesospheric gravity waves in the near infrared OH, O2(0,1) and the visible OI(557.7 nm) nightglow emissions have been made from Bear Lake (BLO) Observatory, Utah (41.6° N, 111.6°W).The image data were obtained over a 2-year period (2002-2003) have been used to investigate the occurrence and properties of undular mesospheric bore events. It was detected about 130 events like mesospheric bore during this observation period. The complementary effect determined by the Dewan and Picard model (1998) for the airglow images (OH, O2 e OI557) can be classified in four categories: Brighter Brighter Brighter (BBB), Brighter Brighter Darker (BBD), Brighter Darker Darker (BDD) and Darker Darker Darker (DDD). The BDD effect was most common at Bear Lake (~35%), in this case the bore height is below the OI5577 and O2 layers but above the OH layer. The bore events characteristics retrieved from the image data for BLO also are compared whit results of the low latitude

GWM-02 Gravity wave sources and spectra appearing in a mesoscale model simulation of the Maritime Continent - by Alexander Hassiotis

Status of First Author: Student IN poster competition PhD

Authors: Alexander Hassiotis

Abstract: The Maritime Continent, consisting of north Australia, New Guinea, and the Indonesian archipelago has emerged as an important source region for atmospheric gravity waves (GWs). It is generally thought that in this region the GWs are generated primarily by deep cumulus convection. Simulations with cloud-resolving models have associated deep convection with waves characterized by high frequencies and long vertical wavelengths. Ray-tracing techniques have shown that these waves are favored to reach high altitudes where their influence may be very significant on spatial and temporal scales consistent with their generation. Recent space-based observations have correlated wave variances in the middle atmosphere with the convective zones

in the tropics. The Maritime Continent in particular showed high variances during the wet season, suggesting wave generation by deep convection. Next generation numerical weather prediction models can strongly aid the fast improving satellite measurements by providing important source information and resolving gravity wave source spectra. The synergy between remote sensing platforms and next generation mesoscale models holds much promise for a more complete description of gravity wave source spectra, source distributions, and propagation properties directly relevant to middle atmospheric studies of gravity wave effects. This poster presents a simulation of the Maritime Continent on 17 November 2001 using the Weather Research and Forecasting model to investigate the organization and spectra of potential GW sources in this convectively active system of complex land-sea interactions.

GWM-03 Effects of dynamic atmospheric structure on ducted gravity wave propagation - by Jonathan Snively

Status of First Author: Student IN poster competition PhD

Authors: Jonathan B. Snively (jbs231@psu.edu), Victor P. Pasko (vpasko@psu.edu)

Abstract: It is well-known that large-scale atmospheric wave dynamics have a significant affect on, and are likewise affected by, the propagation and dissipation of smaller-scale gravity waves [e.g., Fritts and Alexander, Rev. Geophys., 41 (1), 1003, 2003; Fritts et al., JGR, 68 (3-5), 247, 2006 and references cited therein]. Thermal and wind structure associated with large scale waves and tides may provide ducts for gravity waves of very short period [e.g., Snively et al., JGR, 112 (¬A03304), 2007, and references cited therein]. Such ducted waves may propagate over long horizontal distances, exerting influence far from their original source location. However, propagation of these ducted waves is simultaneously affected by large-scale dynamics. Time-varying wind velocity and atmospheric stability will directly result in changes to duct thickness, duct altitude, and trapped wave characteristics. Using simple theoretical and numerical models [e.g., Snively et al., 2007], effects of time-varying winds on gravity wave ducting are predicted and explored for idealized thermal- and Doppler-ducted waves. These dynamics may be associated with upward or downward vertical phase progression of tides or large-scale waves, and consequently modify the spatial distribution of ducted wave energy, intrinsic wave parameters, and wave intensity over long propagation ranges. These processes, and resulting effects, are explored numerically. Model calculations of hypothetical airglow signatures for such events are obtained, and discussed in comparison with recent observations [e.g., Snively et al., 2007].

GWM-04 Measuring mesopause region nighttime gravity wave zonal momentum flux and tidal influence over Fort Collins, CO (41N, 105W) with Colorado State University Na lidar - by Phillip E. Acott

Status of First Author: Student IN poster competition PhD

Authors: Phillip E. Acott, acott@lamar.colostate.edu, David A. Krueger, Krueger@lamar.colostate.edu, Chiao-Yao She, JoeShe@lamar.colostate.edu, Physics Department, Colorado State University, Fort Collins, CO 80523-1875, Steven C. Reising, Steven.Reising@ColoState.edu, Electrical and Computer Engineering Dept., Colorado State University, Fort Collins, CO 80523-1373

Abstract: In May 2002 the sodium lidar at Colorado State University upgraded from a one-beam to a two-beam system with 35 cm telescopes resulting in semi-regular observations of mesopause region temperature, zonal and meridional winds on a 24-hour continuous basis. In August 2006 two 76 cm telescopes were added. The use of dual beam geometry with 76 cm diameter mirrors has led to sufficient signal-to-noise for the nighttime measurement of zonal momentum flux in the mesopause region from September to April, when the atomic sodium abundance is high. Since the system upgrade over 150 hours of night-time three-beam observations have been made, with a beam geometry of East-West dual beams 20o from zenith using 76 cm telescopes and a North beam 30o from zenith using a 35 cm telescope. Of those measurements four data sets are greater than 24 hours in duration, using a 35 cm telescope North 30o from zenith and a 76 cm telescope East 20o from zenith, with atomic vapor Faraday filters, for daytime measurements. This allows determination of nighttime gravity wave zonal momentum flux with simultaneous 24- hour measurements of the mean and tidal fields of mesopause region temperature, zonal and meridional winds. Such a data set can provide not only the vertical profile of nighttime momentum flux but could also shed light on the accompanying tide-gravity wave interactions. Initial results of this new measurement at Colorado State University will be reported.

GWM-05 Gravity Wave Instability Dynamics at High Reynolds Numbers - by Ling Wang

Status of First Author: Non-student PhD

Authors: Ling Wang, David Fritts, Joe Werne, Tom Lund, and Kam Wan, NorthWest Research Associates, Colorado Research Associates Division

Abstract: We conducted direct numerical simulations to examine gravity wave instability dynamics at a high intrinsic frequency, wave amplitudes both above and below nominal convective instability, and a Reynolds number sufficiently high to allow a fully-developed turbulence spectrum. Results reveal strong wave breaking for both wave amplitudes, severe primary wave amplitude reductions within ~ 1 or 2 wave periods, an extended inertial range of turbulence, significant excitation of additional wave motions having upward and downward propagation, and a net positive vertical potential temperature flux due to the primary wave motion, with secondary waves and turbulence contributing variable and net negative potential temperature fluxes, respectively. Turbulence maximizes within ~ 1 buoyancy period of the onset of breaking, arises almost entirely due to shear production, decays rapidly following primary wave amplitude decay, and exhibits significant anisotropy with increasing wavenumber and time. Secondary waves were found to be excited by wave-wave interactions and the turbulence dynamics accompanying wave breaking and to have lower frequencies and smaller momentum fluxes than the primary wave following breaking.

GWM-06 Three dimensional tomography of mesospheric airglow - by D. Scott Anderson

Status of First Author: Student IN poster competition PhD

Authors: D. Scott Anderson, Gary R. Swenson

Abstract: In May and June 2007, the remote sensing department at the University of Illinois at Urbana-Champaign deployed four OH airglow imagers at strategic locations throughout Illinois and Indiana in order to collect data that will be used to tomographically reconstruct to the perturbations on the mesospheric airglow due to atmospheric gravity waves.

GWM-07 Comparison of Atmospheric Waves Observed by All-Sky Cameras of Mt. Bohyun in Korea and Shigaraki in Japan - by Tae-yong Yang

Status of First Author: Student NOT in poster competition Masters

Authors: T.-Y. Yang1, J.-H. Kim1, J.-K. Chung2, Y.-I. Won3, B.-Y. Lee4,K. Shiokawa5, Y.H. Kim1
1Dept. of Astronomy and Space Science, Chungnam National University, Daejeon, Korea
2Korea Astronomy and Space Science Istitute, Daejeon, Korea
3Dept. of Physical Science, Embry-Riddle Aeronautical University, FL, USA
4Korea Polar Research Institute, Incheon, Korea
5Solar-Terrestrial Environment Laboratory, Nagoya University, Toyokawa, Japan

Abstract:

We have carried out all-sky imaging the airglow layers of OH Meinel, O_2 Atmospheric and OI 557.7nm in the period of July, 2001 though September, 2005 at Mt. Bohyun, Korea(36.2˚ N, 128.9˚ E, Alt=1124m). Solar Terrestrial Environment Laboratory of Nagoya University in Japan have also been obtaining similar all-sky images at Shigaraki(34.9˚ N, 136.1˚ E) and other observatories since 1998. The all-sky images of Mt. Bohyun often show horizon to horizon wave crests, known as band type waves, and we found that their wavelengths, periods, and seasonal variation in propagation directions are consistent with characteristics of gravity waves filtered by winds at intermediate altitudes. By applying specific selection criteria of waves and cloud coverages to the all-sky images, we derived monthly occurrence rates for the band type waves, and found that the waves occurred least in March and September at Mt Bohyun. It is interesting to note a recent suggestion by lidar observations in Brazil that tidal activities are minimized in equinoxes and may be related to wave activities at the airglow altitudes. In order to test this suggestion on global nature for the generation of waves seen in airglow layers, we compare all-sky images at Mt. Bohyun and Shigaraki. For proper comparison, we apply the same method and criteria to Shigaraki's images as to Mt Bohyun's. We will present similarities and differences in terms of seasonal distributions of wavelengths, periods, propagation directions and occurrences of waves observed in both countries, which may help see whether airglow waves are more related to low altitude sources such as orographic and convective disturbances in the troposphere or to in situ sources in the mesosphere such as mesosphere wind shear or secondary wave formation.

Sprites, Jets, and Lightning

SPR-01 Physical Mechanisms of Blue Jets and Gigantic Jets - by Jeremy Andre Riousset

Status of First Author: Student IN poster competition PhD

Authors: Jeremy A. Riousset and Victor P. Pasko, CSSL Laboratory, The Pennsylvania State University, University Park, Pennsylvania, USA. (jar471@psu.edu; vpasko@psu.edu), Paul R. Krehbiel, Ronald J. Thomas and William Rison
New Mexico Institute of Mining and Technology, Socorro, New Mexico, USA (krehbiel@ibis.nmt.edu; rison@ee.nmt.edu; thomas@nmt.edu)

Abstract: A long-standing question in lightning studies concerns the mechanisms for propagation of lightning discharge outside the thundercloud. This question appears to be directly relevant for understanding recently discovered blue jet and gigantic jet phenomena, which provide direct path of electrical contact between thundercloud tops and the mesospheric and lower ionospheric regions. The development of lightning discharge inside or outside the thundercloud is most likely related to two fundamental factors, the cloud electrical configuration at the moment of the initiation of the lightning and the locus of this initiation. Unfortunately, loci of initiation of discharges as common as negative cloud-to-ground lightning (–CG) are still debated [Uman, The Lightning Discharge, Dover, Mineola, NY, 2001, p. 10; Rakov and Uman, Lightning: Physics and Effects, Camb. Univ. Pr., Cambridge, U.K., 2001, p. 111], and therefore reasons why a lightning would develop as an intracloud flash or as a cloud-to-ground flash remain unclear. The recent discovery of blue jets [Wescott et al., GRL, 22(10), pp. 1209–1212, 1995; Sentman et al., GRL, 93(20), pp. 2857–2860, 1995; Boeck et al., JGR, 19(99), p. 1992, 1995] and gigantic jets [Pasko et al., Nature, 416, pp. 152–154, 2002; Su et al., Nature, 423, pp. 974–976, 2003] raised again the question of the propagation of discharge channels outside of the thundercloud. Both blue jets and gigantic jets are ionization channels propagating upward from the cumulonimbus top up to altitudes ~30–40 km and ≥70 km, respectively. These two phenomena are believed to be initiated as regular lightning leaders [Petrov et al., Tech. Phys., 44, pp. 472–475, 1999]. Indeed, recent observations [Wescott et al., JASTP, 60, pp. 713–724, 1998; JGR, 106(A6), pp. 10,467–10,478, 2001; Lyons et al., BAMS, 84(4), pp. 445–454, 2003] favor the hypothesis of the streamer nature of these jets, and further support the hypothesis of their initiation as regular lightning leader channels as first suggested in [Petrov et al., 1999]. In this work, we show that a direct physical analogy can be established between cloud-to-ground discharge as leader channels exiting the cloud downward, and the jet phenomena in which lightning leader channels exit the cloud upward. We further discuss possible mechanisms explaining both propagation of lightning discharge to the ground and initiation of jet discharges.

SPR-02 Investigating Sprite Halo Optical Signatures and Associated Lightning Characteristics over South America - by Matthew Bailey

Status of First Author: Student IN poster competition PhD

Authors: M. Bailey, M. J. Taylor, P. D. Pautet, Utah State University, S. Cummer, J. Li, N. Jaugey, Duke University
J. Thomas, R. Holzworth, University of Washington, F. Sao Sabbas, O. Pinto, INPE, N. Schuch, CRSPE/INPE

Abstract: As part of the southern Brazil sprite campaign in summer 2006, almost 600 transient luminous events (TLE's) were imaged from two large thunderstorms over north-eastern Argentina on February 22-23 and March 3-4, 2006. These ground-based measurements were made from the Southern Space Observatory (SSO) using an array of intensified CCD cameras arranged to view the low-elevation sky over the extensive storm systems. This poster deals with the 100+ halos and sprite halos imaged on February 22 - 23, and their associated polarity, and when possible, their charge moments, as determined by an ELF VLF lightning sensor also deployed at the SSO.

SPR-03 NO Chemistry and NO-gamma Emissions Associated with Sprite Streamers - by Ningyu Liu

Status of First Author: Non-student PhD

Authors: Ningyu Liu (nul105@psu.edu) and Victor Pasko (vpasko@psu.edu), The Pennsylvania State University, Communications and Space Sciences Laboratory, University Park, PA 16802, USA

Abstract: Driven by lightning discharges during thunderstorms, sprites are one of the manifestations of the upward coupling of electromagnetic energy from tropospheric altitudes to the mesospheric and lower ionospheric regions. Fee electrons are heated/accelerated in sprite discharges [e.g., Pasko et al., JGR, 102, 4529, 1997] and in particular, in the tips of sprite streamers (filamentary components of sprites). Some of them obtain sufficient energies to excite, dissociate and ionize neutral molecules in air (N2 and O2). As a result, chemically active species (e.g., atomic N and O) are generated, and they can initiate a chain of reactions leading to production of several minor but important constituents in the upper atmosphere.

The emissions from excited neutral or ionized particles during sprite discharges are a key indicator of electron energetics of sprite streamers and the involved chemical processes. The spectrum of sprites is known to span in the wavelength range from far-UV (FUV) to infrared. It was assumed that the FUV emissions associated with sprites are from N2 LBH band system [Mende et al., in Sprites, Elves and Intense Lightning Discharges, vol. 225, edited by M. Füllekrug and E. A. Mareev and M. J. Rycroft, pp. 123—149, 2006, Liu and Pasko, GRL, 32, L05104, 2005, Liu et al., GRL, 33, L01101, 2006]. However, laboratory experiments at ground pressure suggest that NO-gamma emissions can be also generated during streamer discharges, which have a wavelength range overlapping with that of N2 LBH emissions [Simek et al., J. Phys. D: Appl. Phys., 35, 2591, 1998; Tochikubo and Teich, Jpn. J. Appl. Phys., 39, 1343, 2000; Ono and Oda, J. Appl. Phys., 97, 013302, 2005].

A model is developed to explore NO chemistry in streamer discharges with particular emphasis on the study of NO-gamma emissions originating from these discharges in air at different pressures. The modeling results indicate that the excited species leading to NO-gamma emissions, NO(A2 ∑+), in sprite streamers at 70 km altitude are mostly produced by interaction of N2(A3 Σu+) metastables with high-density ambient NO(X2 ∏r) molecules. Analysis of the production and loss mechanisms for the upper excited states leading to NO-gamma emissions and N2 LBH emissions demonstrates that the total intensity of NO-gamma emissions associated with sprites is substantially weaker than that of the N2 LBH emissions. The same conclusion can be drawn for elves following similar analysis. It is demonstrated that the presented modeling approach and analysis are consistent with prior knowledge on NO-gamma emissions from aurora, indicating that to observe the NO-gamma emissions from aurora, the ambient NO density must be highly enhanced in the auroral region.

SPR-04 Testing of Sprite Initiation Mechanism with High Time Resolution Lightning and Sprite Measurements - by Jingbo Li

Status of First Author: Student IN poster competition PhD

Authors: Jingbo Li, Steven A. Cummer, Electrical and Computer Engineering Department, Duke University, Durham, North Carolina, USA, Walter A. Lyons, Thomas E. Nelson, FMA Research, Inc., Yucca Ridge Field Station, Ft. Collins, CO 80524, USA

Abstract: Simultaneous measurements of high altitude optical emissions and the magnetic field produced by sprite-associated lightning discharges enable a close examination of the link between low altitude lightning process and high altitude sprite process. In this work, we report results of the coordinated analysis of high speed (1000--10000 frames per second) sprite video and wideband (0.1 Hz to 30 kHz) magnetic field measurements made simultaneously at the Yucca Ridge Field Station and Duke University during the June through August 2005 campaign period. During the observation period, the high speed camera detected 83 sprite events corresponding to 67 +CGs. 46% of these sprite events are delayed more than 10 ms after the lightning return stroke. With the estimated lightning source current moment waveform, we employ a 2-D FDTD model to numerically simulate the electric field at different altitudes and compare it with the breakdown field for short delayed sprite, long delayed sprite, and complicated transient luminous event (TLE) sequences. The simulation results reveal the effect of electric field dependence of the electron mobility. This nonlinearity increases both the amplitude and altitude of the maximum normalized quasi-static electric field above the thundercloud. Our examples also show that sferic burst and slow intensification are always accompanied. The slow intensification plays an important role in the sprite initiation for the long delayed sprites, where the lightning return stroke is not big enough to initiate a sprite. The presence of slow intensification make the electric field easier to accumulate and thus initiate a sprite. For the 10 short delayed sprites and 10 long delayed sprites analyzed, the simulation result with effect of nonlinearities shows good agreement in sprite initiation altitude with measured data.

SPR-05 Data Reporting and case study of a "Bright" Negative Cloud-to-Ground natural lightning event measured by the Thunderstorm Energetic Radiation Array (TERA) during summer 2005 - by Ziad Saleh

Status of First Author: Student IN poster competition PhD

Authors: *Saleh, Z (zsaleh@fit.edu) ; Dwyer, J R (jdwyer@fit.edu) ; Rassoul, H K (rassoul@fit.edu), Florida Institute of Technology, Department of Physics and Space Sciences, 150 W. University Blvd., Melbourne, FL 32901 United States
Uman, M A (uman@ece.ufl.edu) ; Rakov, V (rakov@ece.ufl.edu) ; Howard, J (ironjoe@ufl.edu) ; Jerauld, J (jjerauld@ufl.edu) ; Olsen, R (rco3@ufl.edu), University of Florida, Department of Electrical and Computer Engineering, Gainesville, FL 32611 United States

Abstract: The Thunderstorm Energetic Radiation Array (TERA) is an array of instruments consisting of pairs of x-ray detectors for measuring x-rays and gamma-rays from thunderstorms and lightning. The array is being placed at the University of Florida/Florida Tech International Center for Lightning Research and Testing (ICLRT) at Camp Blanding, FL. As of 2006, 20 instruments have been deployed. When fully operational at the end of the summer of 2007, TERA will consist of a total of 32 instruments. So far, several rocket-triggered and natural cloud-to-ground lightning flashes have been observed that are accompanied by strong bursts of x-rays. In particular, a negative Cloud-to-Ground lightning strike measured in summer 2005 was observed to be unusually bright when measured in x-rays. This event was characterized by 4 return strokes with intense x-rays fluxes measured on several array elements. In this study we will discus some of the characteristics of this event, giving insight into the mechanism by which these x-rays are generated by lightning.

Stratosphere Studies and Below

STR-01 Determination of the Kinematic Momentum Flux in the Boundary Layer: Comparison between the Three-, Four-Beam Methods (DBS), Multi Radar Experiment obtained with a virtual Boundary Layer Radar, and the "ground-truth" obtained from the LES - by Danny Scipión

Status of First Author: Student NOT in poster competition PhD

Authors: Danny Scipion

Abstract: The vertical flux of the horizontal momentum in the boundary layer is usually measured using a Boundary Layer Radar (BLR), and processed from the Doppler Beam Swinging (DBS) technique. Two methods are commonly used: one using three-beam, one vertical and two oblique, and the other using four beams, two pairs of oblique beams symmetrically offset from the vertical.

In the present study a set of virtual radars are generated based on Large-Eddy Simulations (LES), which have been extensively probed for studies of the Boundary Layer. These radars are designed to operate at 915 MHz, and the five beams for the DBS are pointing 20º off vertical pointing to the N, S, E, W and vertical, and will be used to retrieved the fluxes using the three- and four-beam method.

Another approach include four new virtual radars located symmetrically within the LES domain pointing to the same resolution volume at height spaced 100 m, which are called Multi Radar Experiment (MRE). Using a similar approach as the DBS technique the fluxes can be also retrieved.
Finally, the two techniques are compared with the "ground-truth" fluxes obtained from the LES.

STR-02 Gravity Waves in the Lower Stratosphere at South Pole - by Zhenhua Li

Status of First Author: Student NOT in poster competition PhD

Authors: Zhenhua Li, Walter Robinson, Alan Liu

Abstract: We characterize gravity waves in the lower stratosphere at South Pole using high-resolution balloon soundings from 2001 to 2005. A comprehensive analysis is performed for the gravity-wave energy density, vertical wavenumber spectra, and stability. The relations between the background structure of temperature and wind and the gravity wave perturbations at South Pole

are examined. Our results show that gravity wave perturbations in the lower stratosphere are strongest in May and September and weakest in the austral summer. We also explore the relation between the gravity waves and the synoptic-scale variations in the troposphere, which are expected to be a significant mechanism for gravity-wave generation. Then ray-tracing model is used to explore the relation between gravity wave propagation and background field. The minimum of gravity wave activity at South Pole in the austral summer may due to the combination of weaker generation from synoptic activity and unfavorable background field for gravity wave propagation.

STR-03 Observational Study of the Arctic Middle Atmosphere Using Rayleigh Lidar Data - by Brentha Thurairajah

Status of First Author: Student IN poster competition PhD

Authors: Brentha Thurairajah, V. Lynn Harvey, Kazuyo Sakanoi, Kohei Mizutani, Richard L. Collins

Abstract: Rayleigh lidar observations have been made at Poker Flat Research Range (PFRR), Chatanika, Alaska (65oN, 147oW) on an ongoing basis since November 1997. A monthly mean climatology using a nine year Rayleigh lidar data set from 1997-2005 has been developed. These observations made in fall, winter, and spring have yielded a total of approximately 915 hours of nighttime temperature measurements of the middle atmosphere (~40-80km) in the western Arctic. This temperature climatology is compared with other available high latitude data sets from observations and empirical models. The results show that the temperature variability during the northern hemisphere winter months is larger compared to summer months. This variability that can be attributed to the influence of gravity and planetary waves, tides, and the structure, position, and evolution of the polar vortex and anticyclone is being analyzed as a case study using the January 2003 data. This analysis provides a foundation for the proposed observational and modeling study of the Arctic stratosphere and mesosphere Pan-Arctic Study of the Stratospheric and Mesospheric Circulation, (PASSMeC) during the International Polar Year (IPY).

Instruments or Techniques for Middle Atmospheric Observation

ITM-01 ION 1 & 2: Utilizing CubeSat-class Satellites to Perform Optical Remote Sensing Atmospheric Measurements - by Purvesh Thakker

Status of First Author: Student IN poster competition PhD

Authors: Purvesh Thakker, Gary Swenson, Lara Waldrop

Abstract: With a growing secondary payload launch infrastructure, CubeSat-class satellites (1 to 3 kg) provide a unique opportunity to perform low cost space remote sensing and in-situ atmospheric measurements. This work describes the optical remote sensing capabilities and limitations of these satellites with examples from the Illinois Observing Nanosatellite (ION) 1 and 2 programs. ION-1 measures molecular airglow emissions from the O2 Atmospheric band (0,0) at 762 nm which originates from an altitude of ~94 km. Similarly, ION-2 measures atomic hydrogen emission at 656.3 nm originating from the Earth's geocorona.

ITM-02 Mobile Fe-Resonance/Rayleigh/Mie Doppler Lidar: Theoretical Analysis and Instrument Design - by Xinzhao Chu

Status of First Author: Non-student

Authors: Xinzhao Chu, Wentao Huang, Jonathan S. Friedman, and Jeffrey P. Thayer

Abstract: Global temperature, wind and aerosol profiling through the middle and upper atmosphere with high accuracy, precision, and resolution is crucial in the global atmosphere study and improvement of general circulation models. In this paper, we discuss the principle, simulation, design, and potentials of a proposed Fe-resonance/Rayleigh/Mie Doppler lidar that has compelling reasons to be an attractive for these purposes. The proposed lidar integrates the state-of-the-art technologies of lasers, laser spectroscopy, electro-optics, and sensors into a single system to produce a powerful and robust tool with unmatched measurement capabilities. This lidar will provide simultaneous measurements of temperature (30-110 km), wind (80-110 km), Fe density (75-115 km), and aerosol (10-100 km) in both day and night with high accuracy, high precision, and high spatial and temporal resolutions. Chirp-free and dither-free frequency locking and saturation-free Fe layer resonance results in a bias-free estimate of winds and temperatures, which is revolutionary for Doppler lidar. High energy and the UV wavelength employed by the lidar leads

to a much more sensitive estimate of temperature and aerosol backscatter in stratosphere and mesosphere than determined through Na and K lidars. The 80-cm multi-telescope receiver, double-etalon filter for high rejection of solar background, and a state-of-the-art diagnostic system ensures accurate measurements in both day and night. The resulting breakthrough in lidar technology will push the atmospheric observations to a completely new level and the mobility of the system with enable new scientific endeavors.

ITM-03 First Light for the Spatial Heterodyne Spectrometer to Detect Thermospheric Neutral Oxygen Density via Bowen Fluorescence at 844.6 nm - by Steven Watchorn

Status of First Author: Non-student PhD

Authors: Steven Watchorn (Scientific Solutions, Inc., steve@sci-sol.com), John Noto (Scientifc Solutions, Inc., noto@sci-sol.com), Lara Waldrop (University of Illinois - Urbana-Champaign; lwaldrop@uiuc.edu), Michael Migliozzi (Scientific Solutions, Inc., migliozzi@sci-sol.com)

Abstract: This project involves the spectroscopic observation of neutral oxygen via Bowen fluorescence at 844.0 nm using the Spatial Heterodyne Spectrometer. This will allow for the determination of neutral oxygen densities in the thermopshere, and for improved forward modeling of the dynamics of that important region between 250 and 500 km (where neutral oxygen is the dominant species). The values for the neutral oxygen density will be derived from the observations following the technique developed by Dr. Redgie Lancaster. The specific relations between O and O+ in the thermosphere and ionosphere -- involving charge exchange equilibrium and ion energy balance -- will be constrained with this data. The data will also probe the inferred discrepancy between the neutral oxygen density values calculated from O I airglow observations at 6300 Angstroms and those calculated from MSIS theory.

The Spatial Heterodyne Spectrometer (SHS) is a novel kind of interferometer, capable of high-resolution spectroscopy without internal scanning mechanisms. It thus combines the etendue and compactness advantages conventional interferometers (such as the Michelson and Fabry-Perot) enjoy over slit spectrometers with a greatly increased robustness that makes it particularly suited to studies from space platforms or in harsh environments on Earth. Such applications in astronomy and atmospheric science are now being developed.

The SHS developed for this project has been installed and aligned, and is being calibrated, at Millstone Hill Observatory as of May 1st, 2007, and will begin Bowen fluorescence observations in May. The expected signal strength is in the range of a few to tens of Rayleighs, observed around sunset, and the SHS will observe it with a signal-to-noise ratio of 600, including a 3-Angstrom narrowband filter.

ITM-04 A Faraday Filter-Based Spectrometer to Measure Sodium Nightglow D2/D1 Ratios - by Sean Harrell

Status of First Author: Student IN poster competition PhD

Authors: Sean Harrell, C.-Y. She, Titus Yuan, David A. Krueger, and Steven Reising Colorado State University

Abstract: The Chapman mechanism (1939) offers the accepted chemical pathway for the production of excited states for mesospheric sodium that leads to nightglow at two wavelengths: D2 (589.158 nm) and D1 (589.756 nm). While the Chapman mechanism leaves open the possibility that the intensity ratio of the two transitions varies, measurements by Sipler and Biondi (1978) fixed the value at 2. Recent work by Slanger et al. (2005), however, showed that not only does the intensity ratio vary, but its value is related to the concentration ratio of atomic oxygen (O) to molecular oxygen (O2). In this poster, we will describe the design of a compact, Faraday filter-based spectrometer to measure the D2-to-D1 intensity ratio of the sodium nightglow. After this spectrometer is fabricated and deployed at the Colorado State University sodium lidar site, we expect to be able to measure short-term variations of the sodium nightglow intensity ratio, from which the related oxygen concentration ratio can be inferred. These new observations may yield new insights into mesospheric chemistry.

ITM-05 Progress Report for the Boston University Calibration Facility - by Carl Schmidt

Status of First Author: Student IN poster competition Masters

Authors: Schmidt, C. Baumgardner, J.

Abstract: Errors in brightness calibration of optical data affect the entire aeronomy community and are particularly harmful in constraining models of atmospheric processes. In an effort to help provide improved calibration standards, Boston University is currently constructing a facility for common use in the aeronomy community's characterization of interference filters and light sources. The filter analysis portion of this facility consists of a 1m spectrometer operating between 3800 and 8500 Angstroms equipped with a variety of optical components simulating the illumination conditions of a wide array of instrument configurations. Filters up to 4 inches in diameter can be accommodated. Light source calibrations will be performed via two identical, portable, standard spectrometers, one of which is to be distributed about various aeronomy observatories. Both will be periodically calibrated using a Carbon-14 light source at BU to ensure stability. A report on the development of this facility and its instruments is given here.

ITM-06 A Comparison of SCISAT-1 ACE Temperature data in the vicinity of the mesopause with ground-based OH*(3-1) results - by Frank Mulligan

Status of First Author: Non-student

Authors: Mulligan, F. J(1). and R. P. Lowe(2)
(1)National University of Ireland Maynooth, Maynooth, Co. Kildare, IRELAND, frank.mulligan@nuim.ie
(2)The University of Western Ontario, London, Ontario, N6A 3K7, CANADA, rlowe@uwo.ca

Abstract: We report on a comparison of temperatures retrieved by the Atmospheric Chemistry Experiment onboard the Canadian SCISAT-1 satellite for the period January 2004 to May 2006 with temperatures obtained from the OH*(3-1) Meinel band which were recorded more than a decade earlier at 53°N. To facilitate the comparison, we computed an "OH-equivalent temperature" for each ACE temperature profile. The annual cycle of temperature at mesopause altitudes is well reproduced and excellent agreement is obtained in the absolute value of the temperature minimum (~162 K) and in its time of occurrence in the cycle. A significant divergence is observed in mid-winter however, with the ACE OH equivalents more than 20 K less than the ground-based measurements. Results from ground stations at similar latitudes during the same time period appear to confirm the validity of the OH*(3-1) data. Lowering the peak altitude of the weighting function used to compute the OH-equivalent temperatures reduces the temperature difference but the peak would have to be placed at an unrealistically low altitude to achieve complete agreement. This suggests to us that further work may be required on the validation of the ACE temperatures at the upper end of the altitude range in winter conditions.

ITM-07 Development of a Kalman Filter-Based Triangulation Procedure for Sounding Rocket Chemical Release Wind Measurements – by Justin Edward Ingersoll

Status of First Author: Student NOT in poster competition Masters

Authors: Justin Edward Ingersoll and Miguel Larsen

Abstract: Knowledge of the movement of the neutral atmosphere is a key component in any study of the ionosphere. This is especially true with sounding rocket flights as it is not practical to take direct measurements of neutral winds with onboard instruments. Chemical releases from sounding rockets - typically trimethyl aluminum (TMA) - provide this capability by providing a tracer of the motion of the neutral atmosphere at altitudes in D and E region. The resultant chemiluminescent trail is photographed from at least two locations to track its neutral wind-driven movements. Triangulation of these photographs then yields position information at different points in time, which can be combined to obtain a neutral wind profile. The goal of the study described here is to improve the existing triangulation technique by implementing a Kalman filter-based tracking and estimation algorithm. This will allow for a more rigorous and statistically robust calculation of wind profiles based on modern tracking algorithms. The poster describes the scheme and the planned implementation of the procedure, as well as the work that has been completed so far, especially in the automation of various steps in the analysis.

Index